Seismic imaging of subduction zone metamorphism

Stéphane Rondenay
Department of Earth, Atmospheric, and Planetary Sciences, Massachusetts Institute of Technology,
Cambridge, Massachusetts 02139, USA
Geoffrey A. Abers
Department of Earth Sciences, Boston University, Boston, Massachusetts 02215, USA
Peter E. van Keken
Department of Geological Sciences, University of Michigan, Ann Arbor, Michigan 48109, USA

ABSTRACT

Combined analysis of high-resolution seismic images of the Alaska and Cascadia subduction zones reveals where metamorphic fluids are released. Both images show the subducted oceanic crust as a dipping low-velocity layer with a clear termination depth. However, in Alaska the crust is thicker (15–20 km compared to 8 km) and terminates at greater depth (120 km compared to 40 km) than in Cascadia. Based on metamorphic reaction estimates and geodynamic models, we demonstrate that the termination depth corresponds to eclogitization of the crust triggered by dehydration of water-bearing minerals, and that the location of this reaction is dependent on the thermal structure of the subducted slab.

Keywords: subduction, oceanic crust, seismic studies, metamorphism, eclogite, water.

INTRODUCTION

Subduction zones transport water into Earth's interior. The subsequent release of this water through dehydration reactions may trigger intraslab earthquakes and arc volcanism, regulate slip on the plate interface, control plate buoyancy, and regulate the long-term budget of water on the planet's surface (e.g., Peacock, 1990). While the seafloor input and arc output of this system can be sampled directly, at least in principle, the transport and release of fluids at depth are mostly investigated through indirect methods such as geodynamic modeling and experimental petrology (e.g., Schmidt and Poli, 1998; Hacker et al., 2003a). These studies show that the contribution of subducted water to the volcanic arc is critically dependent on the thermal structure, distribution of hydration, and petrology of the downgoing plate, none of which is well known.

Recent seismic observations of subduction zones show the presence of a dipping low-velocity layer likely associated with the subducted crust (Abers, 2005). The layer generally extends to depths of 40–150 km and exhibits velocities 5%–15% slower than the surrounding mantle. It is commonly thought to be composed of hydrated metabasalts (Helffrich, 1996) and metastable gabbro (Hacker et al., 2003a), both of which have the appropriate velocities. At high pressures, these mafic rocks convert to higher-velocity eclogite, which cannot be distinguished seismically from mantle peridotites (Hacker et al., 2003a). The disappearance of the low-velocity layer should thus constrain the depth of eclogitization. Unfortunately, most seismic observations of this layer rely on unusual signals that constrain layer velocities, but poorly resolve its spatial extent (e.g., Abers, 2005; Matsuzawa et al., 1986). Clearly, a better knowledge of the spatial extent of this low-velocity layer and how it varies among slabs with different thermal structure would help to better evaluate what it reveals about subduction dynamics.

In this study, we present robust and self-consistent seismic images of two subduction zones exhibiting very different thermal structures, Cascadia and Alaska (Fig. 1). These images allow for the first direct comparison of different subduction zones in this manner. They show that the low-velocity subducted crust disappears at depths consistent with those at which dehydration reactions trigger eclogitization.

A TALE OF TWO SUBDUCTION ZONES

In central Alaska (Fig. 1A), the Pacific plate converges with North America at a rate of ~55 mm/yr (DeMets et al., 1994). The plate is 35–45 Ma in age at the trench (Atwater, 1989), placing it in the midrange of slab thermal structures globally (Kirby et al., 1996). The downgoing slab is fairly continuous beneath the region, as inferred from seismicity (Ratchkovski and Hansen, 2002) and seismic tomography (Eberhart-Phillips et al., 2006). However, it comprises an anomalous Denali segment characterized by (1) largely absent volcanism (although see Nye, 1999), (2) seismicity extending to only 100–150 km depths and not 150–200 km as in the rest of the Alaska-Aleutian system, (3) active mountain building, and (4) a shallow subduction angle (see Fig. DR1 in GSA Data Repository[1]). The unusual nature of this segment may be attributed to the ongoing subduction of the Yakutat terrane (Plafker and Berg, 1994), a composite block that translates with the Pacific plate. Portions of this terrane that have subducted beneath the Aleutian megathrust are imaged by refraction as a 15–20-km-thick subhorizontal layer beneath coastal Alaska (Brocher et al., 1994).

In the Cascadia subduction zone (Fig. 1B), the Juan de Fuca plate subducts beneath western North America at a rate of 35–45 mm/yr (DeMets et al., 1994). Along the trench, the subducting plate is very young (6–10 Ma; Wilson, 2002), placing it at the warm end of plate thermal structures. A Wadati-Benioff zone is observed between 40 and 90 km depth north of 47°N, suggesting a slab dip steepening from 10° to 30° in that region. Conversely, intraslab seismicity is absent in Oregon for reasons that are not well understood (e.g., Wells et al., 2002). Active volcanism, magnetotelluric analyses, and seismic images support the existence of a continuous, dehydrating slab to at least 150–200 km depth (e.g., Rasmussen and Humphreys, 1988; Wannamaker et al., 1989).

SEISMIC IMAGES

Images shown here are constructed by multichannel inversion of scattered teleseismic body waves recorded at dense arrays of broadband seismographs (Bostock et al., 2001). We use data recorded by the BEAAR array in Alaska (Fig. 1A) (Ferris et al., 2003) and the CASC93

---

[1]GSA Data Repository item 2008067, robustness and resolution of the seismic images, and input parameters of thermal models, is available online at www.geosociety.org/pubs/ft2008.htm, or on request from editing@geosociety.org or Documents Secretary, GSA, P.O. Box 9140, Boulder, CO 80301, USA.
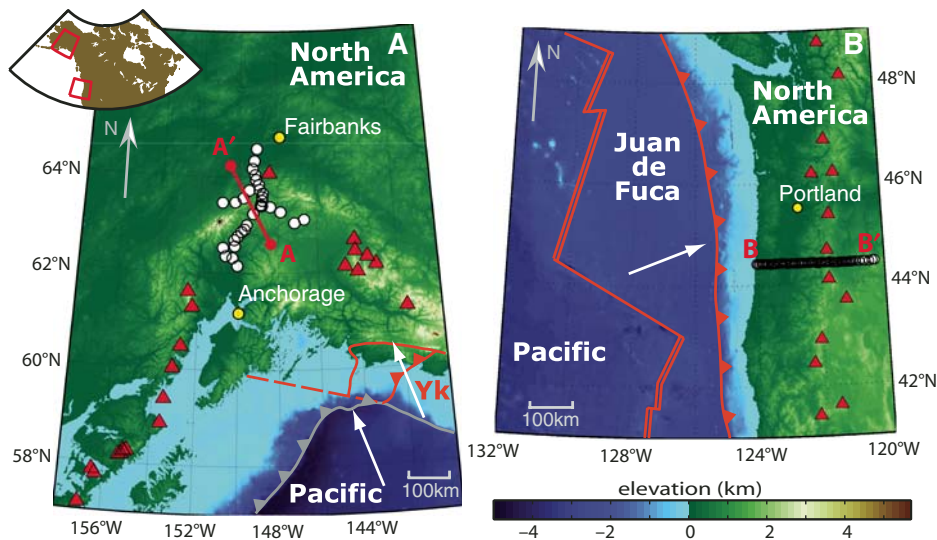
Figure 1. Regional setting of the Alaska (A) and Cascadia (B) subduction zones. Toothed lines show trenches, red triangles show major Quaternary volcanoes, white arrows show plate convergence direction, and white circles show locations of seismic stations. A: Solid gray and orange lines show the surface contacts of the Pacific plate and Yakutat (Yk) terrane (Plafker and Berg, 1994). The dashed orange line marks the southwestern extent of the subducted Yakutat terrane based on aeromagnetic anomaly (from Ferris et al., 2003). Line A–A′ indicates the surface projection of the seismic profile in Figures 2A and 2C. B: Solid orange lines show the outline of the Juan de Fuca plate. Line B–B′ indicates the surface projection of the seismic profile in Figures 2B and 2D.

array in Oregon (Fig. 1B) (Nabelek et al., 1993). Previous applications indicate that the expected volume resolution is 3–4 km for teleseismic signals in the 0.03–0.3 Hz frequency band used here (Rondenay et al., 2005). The applicability of the method is validated separately for Cascadia (Rondenay et al., 2001) and Alaska (see GSA Data Repository).

Three robust features are apparent in the image of central Alaska (Figs. 2A and 2C). First, the Moho is observed as a positive (downward slow-to-fast) velocity gradient across the entire profile at variable depths ranging from 25 to 40 km. These fluctuations generally reflect isostatic compensation of topography in the Alaska Range (Veenstra et al., 2006). Second, an upper-mantle discontinuity is observed at ~60 km depth in the northwest portion of the seismic profile. It is interpreted by Rondenay et al. (2004) as a thermal and/or compositional boundary associated with a sharply defined base of the lithosphere. Third, we observe a dipping, low-velocity layer with thickness ranging from 23 km in the southeast to 12–15 km in the northwest at 50–130 km depth. This low-velocity layer is reminiscent of subducted oceanic crust as imaged elsewhere, although it is significantly thicker than average (usually ~8 km; White et al., 1992), even considering the 3–4 km resolution limit. Colocated receiver functions detected a similar, albeit constant-thickness, layer that was interpreted as the subducted Yakutat terrane (Ferris et al., 2003). The thickness difference between the two results can be reconciled if the top of the low-

velocity layer is bounded by a velocity gradient rather than a discontinuity, while the termination of the dipping low-velocity layer at ~120–130 km depth is a robust feature as supported by Ewald sphere analysis (see GSA Data Repository).

Several robust features are apparent in the Cascadia profile (Figs. 2B and 2D) and have been discussed elsewhere (Rondenay et al., 2001; Bostock et al., 2002). First, the horizontal, positive discontinuity in the central/eastern portion of the profile is interpreted as the continental Moho. Second, a dipping, 7–9-km-thick low-velocity layer observed in the western portion of the model is interpreted as the crust of the subducted Juan de Fuca plate. Third, a disruption of the inferred oceanic crust is observed below the forearc at 40 km depth and is accompanied by a change in dip and signature of the subducting oceanic crust. The velocity increase in the crust has been attributed to eclogitization (Rondenay et al., 2001), and the wide, low-velocity region near the intersection of the plate and the continental Moho was attributed to serpentine alteration (Bostock et al., 2002).

SLAB DEHYDRATION AND METAMORPHISM

The two similar images of two distinct subduction zones provide insight into the links between seismic properties of the slab and its petrological evolution. For each subduction zone, we compare the locus of velocity increase in the crust with the expected petrological changes as a function of P-T paths predicted by geo-

dynamic models (Fig. 3). From this comparison, we observe an overall correspondence between the depths at which dehydration is predicted to occur, in either hydrated metabasalts or serpentinized harzburgites, and the depth range at which the low-velocity channel is observed. Various explanations for this correspondence have been proposed in the literature, but most of them ultimately rely on dehydration triggers for eclogitization. We discuss the four main models below.

First, the low-velocity layer may be subducted crust largely composed of hydrated metabasalt, in which case its disappearance reflects equilibrium dehydration to eclogite. While the predicted pressure for dehydration agrees well with the 40–45 km depth at which the low-velocity crust disappears in Cascadia, the 130 km depth of disappearance beneath Alaska corresponds to temperatures near 600 °C and exceeds temperatures of dehydration predicted by Hacker et al. (2003a). The experimentally derived dehydration curves (Forneris and Holloway, 2003) show closer agreement with the maximum depth of low velocities beneath Alaska. It may be that Hacker et al. (2003a) underestimate dehydration temperatures, but it also may be that metastable blueschists could persist in the absence of free fluids (John and Schenk, 2003).

Second, the low-velocity layer may be subducted crust composed of metastable dry gabbro, in which case its disappearance corresponds to delayed eclogitization (Hacker et al., 2003b). There is no need to invoke metastability of gabbro in Cascadia. The observation of low velocities in the wedge directly above the termination of low velocities in the slab is indirect evidence for hydration-serpentinization of the wedge, so water must be released from the slab (Bostock et al., 2002). In Alaska, the subducted crust has ambiguous origin but may comprise multiple layers: layers of hydrated basalts or sediments that release fluids below 60 km depth where the low-velocity layer tapers, and layers of metastable gabbros that persist to 120 km depth. More generally, the metastability of gabbro is regulated by fluid interaction, in that dry gabbros have been found occasionally well into the eclogite stability field, but gabbros showing evidence of fluid interaction generally react to eclogite (Hacker, 1996). The introduction of water into subducted crust should catalyze the formation of eclogite, presumably as a consequence of dehydration occurring nearby, perhaps in underlying faults where hydrated minerals such as serpentinized peridotite are present. In this scenario, the layers vanish seismically where reactions that release catalyzing fluids occur.

Third, the low-velocity layer may be a serpentinite layer beneath the subducted crust in the underlying mantle (Ranero et al., 2003). While appropriate degrees of serpentinization could produce the 5%–15% velocity reduction
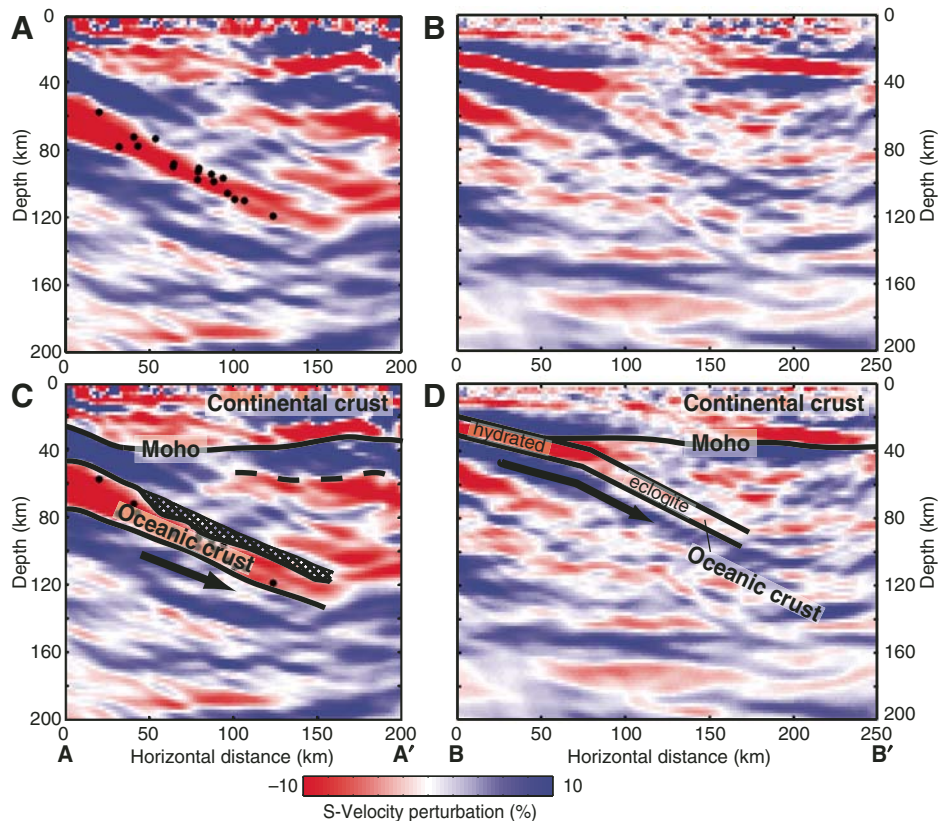
Figure 2. High-resolution seismic images across central Alaska (A and C) and Cascadia (B and D). Upper panels show raw profiles and lower panels show interpreted profiles. Red to blue color scale represents negative (slower) to positive (faster) S-velocity perturbations relative to a one-dimensional background model. In Alaska, seismic velocities in the upper crustal layer (hashed region in Fig. 2C) increase progressively with increasing depth, whereas the lower crustal layer remains relatively unperturbed (uniform low velocity—see GSA Data Repository). Dashed line in panel (C) denotes a continental upper-mantle discontinuity at 60 km depth.

Figure 3. Predicted pressure-temperature (*P-T*) paths for the subducted crust beneath central Alaska (blue shading) and Cascadia (red shading), over phase diagram for hydrated metabasalts of Hacker et al. (2003a)—see this reference for a complete facies description. The thermal model of Alaska is from Abers et al. (2006), and that of Cascadia is modified from van Keken et al. (2002) (see GSA Data Repository for a description of the models). The shading ends at the pressure corresponding to the termination depth of imaged crust. Red and blue lines denote the top (dashed) and base (solid) of the subducted crust. The modeled crust is 20 km thick in Alaska and 7 km thick in Cascadia; the blue dot-dashed line indicates the *P-T* path of the coldest point in the Alaskan crust. The thick dashed lines denote transformation boundaries associated with the largest release of water and the greatest increase in seismic velocity (15%–20%). For hydrated metabasalts, these are estimates of the onset of eclogitization from blueschist and amphibolite at pressures below 1.6 GPa, and from lawsonite breakdown at higher pressures: H03 (field-based; Hacker et al., 2003a) and FH03 (laboratory experiment by Forneris and Holloway, 2003; similar to Schmidt and Poli, 1998). For ultramafic systems, these are the stability limits for serpentine (Serp out) and chlorite (Chl out), both from Hacker et al. (2003a).

associated with the low-velocity layer (e.g., Bostock et al., 2002), a comparison of our two subduction systems argues against this model. We note that in both subduction systems, there is a good match between the thickness of the subducted oceanic crust at depth derived from the teleseismic images, and the thickness of the oceanic crust entering the trench derived from active source profiles (Brocher et al., 1994; Flueh et al., 1998). From one subduction zone to the other, however, the thickness of the subducted oceanic crust is significantly different (~23 km in Alaska versus ~7–9 km in Cascadia in the upper portion of the model). There is no reason why the deep serpentinized layer should be equal in thickness to the oceanic crust entering the trench in each subduction system. Moreover, the crustal (meta)gabbros and/or metabasalts should be stable in the updip portion of both systems, and hence, visible as additional low-velocity material in the seismic image. If the low-velocity layer is interpreted as a serpentinite layer, then where is the crust?

Fourth, the low-velocity layer might be a layer of serpentinite, ponded fluid, or melt overlying the downgoing plate, as recently inferred for northern Honshu (Kawakatsu and Watada, 2007). This explanation is difficult to reconcile with the geometries observed in our images. The observed layer exhibits velocities that are lowest in the updip portion of each profile and gradually increase as the plate subducts, causing the layer to disappear at depth. Conversely, fluid release, serpentine formation, or melt accumulation should result in a layer that grows at depth, at least initially where the dehydration products first encounter the flowing part of the mantle wedge. This should occur at depths greater than ~80 km (Abers et al., 2006), consistent with the inferred serpentinization in Japan (Kawakatsu and Watada, 2007). Moreover, we recall that the layer thickness at depth corresponds to that of the subducted crust at the trench, and that there is little room in the interpretation to accommodate any additional low-velocity material. Therefore, a thin layer of serpentine or melt (<3 km thick) above the subducted crust cannot be ruled out, but it is not the main source of the observed low-velocity signal.

Based on this analysis, it is most likely that the low-velocity layers observed in the teleseismic profiles represent subducted oceanic crust on its path to eclogitization. Whether the crust is heavily hydrated or metastable remains difficult to determine. However, in either case, the release of fluids via dehydration of water-bearing minerals is required to catalyze the transformation to eclogite. In this framework, high-resolution seismic images and dynamical models provide constraints on dehydration reactions that are complementary to those inferred from experimental and field-based thermodynamic considerations alone. They reveal the pattern of these

reactions and the depth at which they occur, and show that dehydration processes dominate the structure of slabs at 40–150 km depth.

REFERENCES CITED

Abers, G.A., 2005, Seismic low-velocity layer at the top of subducting slabs beneath volcanic arcs: Observations, predictions, and systematics: Physics of the Earth and Planetary Interiors, v. 149, p. 7–29, doi: 10.1016/j.pepi.2004.10.002.

Abers, G.A., van Keken, P., and Kneller, E., Ferris, A., and Stachnik, J., 2006, The thermal structure of subduction zones constrained by seismic imaging: Implications for slab dehydration and wedge flow: Earth and Planetary Science Letters, v. 241, p. 387–397.

Atwater, T., 1989, Plate tectonic history of the northeast Pacific and western North America, in Winterer, E.L., et al., eds., The eastern Pacific Ocean and Hawaii: Boulder, Colorado, Geological Society of America, Geology of North America, v. N, p. 21–72.

Bostock, M.G., Rondenay, S., and Shragge, J., 2001, Multiparameter two-dimensional inversion of scattered teleseismic body waves, 1: Theory for oblique incidence: Journal of Geophysical Research, v. 106, p. 30,771–30,782, doi: 10.1029/2001JB000330.

Bostock, M.G., Hyndman, R.D., Rondenay, S., and Peacock, S.M., 2002, An inverted continental Moho and serpentinization of the forearc mantle: Nature, v. 417, p. 536–538, doi: 10.1038/417536a.

Brocher, T., Fuis, G., Fisher, M., Plafker, G., and Moses, M., 1994, Mapping the megathrust beneath the northern Gulf of Alaska using wide-angle seismic data: Journal of Geophysical Research, v. 99, p. 11,663–11,685, doi: 10.1029/94JB00111.

DeMets, C., Gordon, R.G., Argus, D.F., and Stein, S., 1994, Effect of recent revisions to the geomagnetic reversal time-scale on estimates of current plate motions: Geophysical Research Letters, v. 21, p. 2191–2194, doi: 10.1029/94GL02118.

Eberhart-Phillips, D., Christensen, D.H., Brocher, T.M., Hansen, R., Ruppert, N.A., Haeussler, P.J., and Abers, G.A., 2006, Imaging the transition from Aleutian subduction to Yakutat collision in central Alaska, with local earthquakes and active source data: Journal of Geophysical Research, v. 111, B11303, doi: 10.1029/2005JB004240.

Ferris, A., Abers, G.A., Christensen, D.H., and Veenstra, E., 2003, High resolution image of the subducted Pacific (?) plate beneath central Alaska, 50–150 km depth: Earth and Planetary Science Letters, v. 214, p. 575–588, doi: 10.1016/S0012-821X(03)00403-5.

Flueh, E.R., Fisher, M.A., Bialas, J., Childs, J.R., Klaeschen, D., Kukowski, N., Parsons, T., Scholl, D.W., ten Brink, U., Tréhu, A.M., and Vidal, N., 1998, New seismic images of the Cascadia subduction zone from cruise SO108-ORWELL: Tectonophysics, v. 293, p. 69–84, doi: 10.1016/S0040-1951(98)00091-2.

Forneris, J.F., and Holloway, J.R., 2003, Phase equilibria in subducting basaltic crust: Implications for H_2O release from the slab: Earth and Planetary Science Letters, v. 214, p. 187–201, doi: 10.1016/S0012-821X(03)00305-4.

Hacker, B.R., 1996, Eclogite formation and the rheology, buoyancy, seismicity, and H_2O content of oceanic crust, in Bebout, G., et al., eds., Subduction top to bottom: American Geophysical Union Geophysical Monograph 96, p. 337–346.

Hacker, B.R., Abers, G., and Peacock, S., 2003a, Subduction factory, 1: Theoretical mineralogy, density, seismic wave speeds, and H_2O contents: Journal of Geophysical Research, v. 108, 2029, doi: 10.1029/2001JB001127.

Hacker, B.R., Peacock, S.M., Abers, G.A., and Holloway, S.D., 2003b, Subduction factory, 2: Are intermediate-depth earthquakes in subducting slabs linked to metamorphic dehydration reactions?: Journal of Geophysical Research, v. 108, 2030, doi: 10.1029/2001JB001129.

Helffrich, G.R., 1996, Subducted lithospheric slab velocity structure: Observations and mineralogical inferences, in Bebout, et al., eds., Subduction top to bottom: American Geophysical Union Geophysical Monograph 96, p. 215–222.

John, T., and Schenk, V., 2003, Partial eclogitisation of gabbroic rocks in a late Precambrian subduction zone (Zambia): Prograde metamorphism triggered by fluid infiltration: Contributions to Mineralogy and Petrology, v. 146, p. 174–191, doi: 10.1007/s00410-003-0492-8.

Kawakatsu, H., and Watada, S., 2007, Seismic evidence for deep-water transportation in the mantle: Science, v. 316, p. 1468–1471, doi: 10.1126/science.1140855.

Kirby, S., Engdahl, E.R., and Denlinger, R., 1996, Intermediate-depth intraslab earthquakes and arc volcanism as physical expressions of crustal and uppermost mantle metamorphism in subducting slabs, in Bebout, G., et al., eds., Subduction top to bottom: American Geophysical Union Geophysical Monograph 96, p. 195–214.

Matsuzawa, T., Umino, N., Hasegawa, A., and Tagaki, A., 1986, Upper mantle velocity structure estimated from PS-converted wave beneath the northeastern Japan Arc: Geophysical Journal of the Royal Astronomical Society, v. 86, p. 767–787.

Nabelek, J., Li, X.-Q., Azevedo, S., Braunmiller, J., Fabritius, A., Leitner, B., Tréhu, A.M., and Zandt, G., 1993, A high-resolution image of the Cascadia subduction zone from teleseismic converted phases recorded by a broadband seismic array: Eos (Transactions, American Geophysical Union), v. 74, p. 431.

Nye, C., 1999, The Denali volcanic gap—Magmatism at the eastern end of the Aleutian arc: Eos (Transactions, American Geophysical Union), v. 80, no. 46, p. 1203.

Peacock, S.M., 1990, Fluid processes in subduction zones: Science, v. 248, p. 329–337, doi: 10.1126/science.248.4953.329.

Plafker, G., and Berg, H., 1994, Overview of the geology and tectonic evolution of Alaska, in Plafker, G., and Berg, H., eds., The Geology of Alaska: Boulder, Colorado, Geological Society of America, Geology of North America, v. G-1, p. 989–1021.

Ranero, C., Morgan, J.P., McIntosh, K., and Reichert, C., 2003, Bending-related faulting and mantle serpentinization at the Middle America trench: Nature, v. 425, p. 367–373, doi: 10.1038/nature01961.

Rasmussen, J., and Humphreys, E., 1988, Tomographic image of the Juan de Fuca plate beneath Washington and western Oregon using teleseismic P-wave travel times: Geophysical Research Letters, v. 15, p. 1417–1420.

Ratchkovski, N., and Hansen, R., 2002, New evidence for segmentation of the Alaska subduction zone: Bulletin of the Seismological Society of America, v. 92, p. 1754–1765, doi: 10.1785/0120000269.

Rondenay, S., Bostock, M.G., and Shragge, J., 2001, Multiparameter two-dimensional inversion of scattered teleseismic body waves, 3: Application to the Cascadia 1993 data set: Journal of Geophysical Research, v. 106, p. 30,795–30,808, doi: 10.1029/2000JB000039.

Rondenay, S., Abers, G.A., and Ferris, A., 2004, A new, high-resolution seismic profile of the central Alaskan subduction zone [abs.]: Eos (Transactions, American Geophysical Union), v. 85, abstract U54A-05.

Rondenay, S., Bostock, M., and Fischer, K., 2005, Multichannel inversion of scattered teleseismic body waves: Practical considerations and applicability, in Levander, A., and Nolet, G., eds., Seismic Earth: Array analysis of broadband seismograms: American Geophysical Union Geophysical Monograph 157, p. 187–204.

Schmidt, M.W., and Poli, S., 1998, Experimentally based water budgets for dehydrating slabs and consequences for arc magma generation: Earth and Planetary Science Letters, v. 163, p. 361–379, doi: 10.1016/S0012-821X(98)00142-3.

van Keken, P.E., Kiefer, B., and Peacock, S.M., 2002, High-resolution models of subduction zones: Implications for mineral dehydration reactions and the transport of water into the deep mantle: Geochemistry, Geophysics, Geosystems, v. 3, 1056, doi: 10.1029/2001GC000256.

Veenstra, E., Christensen, D.H., Abers, G.A., and Ferris, A., 2006, Crustal thickness variation in south-central Alaska: Geology, v. 34, p. 781–784, doi: 10.1130/G22615.1.

Wannamaker, P.E., Booker, J.R., Jones, A.G., Chave, A.D., Filloux, J.H., Waff, H.S., and Law, L.K., 1989, Resistivity cross section through the Juan de Fuca subduction system and its tectonic implications: Journal of Geophysical Research, v. 94, p. 14,127–14,144.

Wells, R.E., Blakely, R.J., and Weaver, C.S., 2002, Cascadia microplate models and within-slab earthquakes, in Kirby, S., et al., eds., The Cascadia subduction zone and related subduction systems—Seismic structure, intraslab earthquakes and processes, and earthquake hazards: U.S. Geological Survey Open-File Report 02-328, p. 17–23.

White, R.S., McKenzie, D., and O'Nions, R.K., 1992, Oceanic crustal thickness from seismic measurements and rare-earth element inversion: Journal of Geophysical Research, v. 97, p. 19,683–19,715.

Wilson, D.S., 2002, The Juan de Fuca plate and slab: Isochron structure and Cenozoic plate motions, in Kirby, S., et al., eds., The Cascadia subduction zone and related subduction systems—Seismic structure, intraslab earthquakes and processes, and earthquake hazards: U.S. Geological Survey Open-File Report 02-328, p. 9–12.